Korean J. Chem. Eng., 17(5), 600-612 (2000)

Statistical Condensation Adsorption Isotherms of Gas Molecules Adsorbed on Porous Adsorbents, Surface Monolayer Adsorption Isotherms and Hysteresis Phenomena

Daekyoum Kim†

Department of Chemical Engineering, Hanyang University, 17, Haengdang-dong, Sungdong-ku, Seoul 133-791, Korea
(*Received 1 July 2000 • accepted 1 August 2000*)

Abstract−Condensation adsorption isotherms of type IV (or V) according to BDDT classification on porous adsorbents composed of one or two groups of adsorption sites are derived statistically. When β_{c1} (or β_{c2}) is less than unity, the isotherm becomes type IV, and when it is greater than unity, the isotherm becomes type V. It is understood that the negative sign(−) of the additional adsorption energy, q, in the nth layer in deriving those theoretical isotherms plays a decisive role on the horizontally flat approach to the axis of the isotherm near the saturation vapor pressure. The values of the surface area can be calculated easily. The pore radii of all the adsorbents which we have obtained by using the derived isotherms with respect to the appropriately selected experimental data agree with those obtained by using the Kelvin equation. Many surface mono-layer adsorption isotherms are obtained in the process of deriving the various adsorption isotherms. From them we can learn that the surface sites are not adsorbed completely even near the saturated vapor pressure, and we can find the range of error by comparing them with v_ms of the BET equation. We could mention through judging the results of a great deal of the experimental isotherm data of types IV and V that "the cause of hysteresis phenomena of the condensation adsorption-desorption of gases is originated from the deviation from the thermodynamically reversible adsorption-desorption process in the condensation adsorption-desorption of gases."

Key words: Pore Condensation Adsorption Isotherms, Surface Mono-layer Adsorption Isotherms, Hysteresis Phenomena

INTRODUCTION

In the previous literature [Kim, 2000] to get the exact theoretically adsorbed amount of gas molecules on a non-porous adsorbent, we derived the adsorption isotherms and compared them with the experimental data. They were type II adsorption isotherms like the BET equation [Brunauer et al., 1938; Pickett, 1945; Hill, 1946a]. In the present study we derive statistical thermodynamical model equations to describe the condensed adsorbed amount of gas molecules on a porous adsorbent. There is a great deal of experimental data for type IV but a little for type V [Gregg and Sing, 1969]. Until now many theoretical researches [Gregg and Sing, 1969; Brunauer et al., 1940; Hill, 1946b; Rudizinski and Everett, 1992] have been done for the isotherms. Hill [Hill, 1946b] derived the adsorption isotherm on a porous adsorbent by utilizing the partial conception which BDDT [Brunauer et al., 1940] mentioned. BDDT derived type IV and V isotherms kinetically. The conception about the additional energy, q, of the nth layer mentioned in their modeling is used newly in the present study. It can be positive or negative with respect to the liquefied energy of adsorbate molecules. When q has a positive sign, the adsorbate molecules are adsorbed on the wall of the pore, and when it has a negative sign, the adsorbed molecules cause pore plugging by the capillary condensation around the center line of the pore as shown in Fig. 1. In the literature of BDDT it is supposed that this additional energy has the same sign as D_i, D_{s1} or D_{s2} has, where D_i is the adsorption energy from the second to nth layer, or D_{s1} or D_{s2}, the surface adsorption energy. But we think that the nth layer molecules attracted from all walls having the negative sign(−) of q are situated in the center line of the pores, and they with small adsorption energies counteract the surrounding adsorbed molecules. Hence, they have much weaker bonding than their neighbor molecules have and are easily evaporated because the speed at which the adsorption heat is taken away

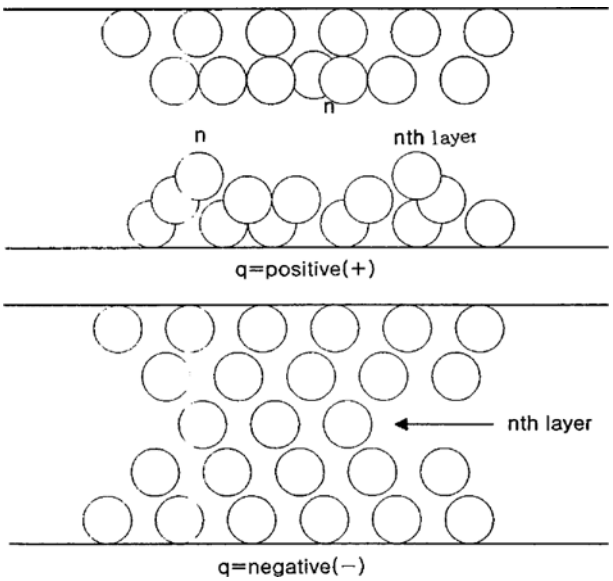

Fig. 1. Schematic description of the adsorption as to the additional energy (q) of the nth layer in the capillary pore.

†To whom correspondence should be addressed.
E-mail: dkkim9744@hanmail.net

is slow. Therefore, we think that the adsorbed molecules on the nth layer should have the additional energy, q, of the negative sign(−) and the adsorption energies of molecules adsorbed on the nth layer are not larger than those of the molecules adsorbed on the neighbor or those of lower layer molecules. Therefore, it is considered that the desorption (evaporation) of the adsorbed molecules starts first from the center molecule in the surface film of the pore. Here we do not consider this in the derivation on the continuous adsorption after the pores are filled by condensation adsorption.

The amount of the adsorbed molecules is considered to increase as the pressure increases because certain harmonized vibrational modes of the adsorbent die out, or the strength of vibrations is reduced, while the electro-negativity coming from the nuclear is not reduced and increases a little.

Hence in this research we derive condensation adsorption isotherms of types IV and V, obtain the surface mono-layer adsorption isotherms additionally for the gas molecules adsorbed on the porous adsorbents composed of 1 and 2 groups of sites, and discuss the cause of the hysteresis phenomena for the adsorption-desorption. The repulsions between the adsorbates are ignored.

STATISTICAL MODELINGS

1. Capillary Condensation Adsorption Isotherm for the Gas Molecules Adsorbed on the Porous Adsorbent Composed of 1 Group of Sites

Let us assume that the porous adsorbent is composed of a number of capillaries, they are formed of two flat walls, the adsorption occurs both on the free surface and among the capillary walls, and the capillaries are plugged by condensation. But it is supposed that the pore is composed of 1/m flat walls since more than two flat

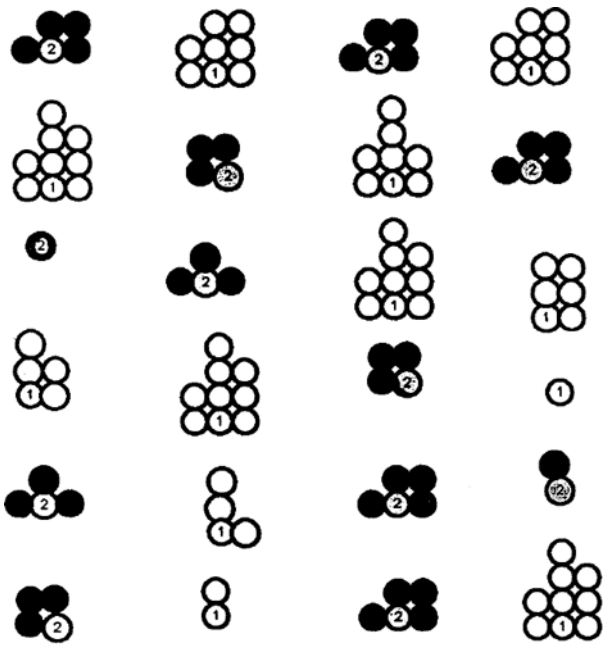

Fig. 2. Schematic statistical distribution of sites of groups 1 and 2 concerning about the stronger of group 1 than group 2.

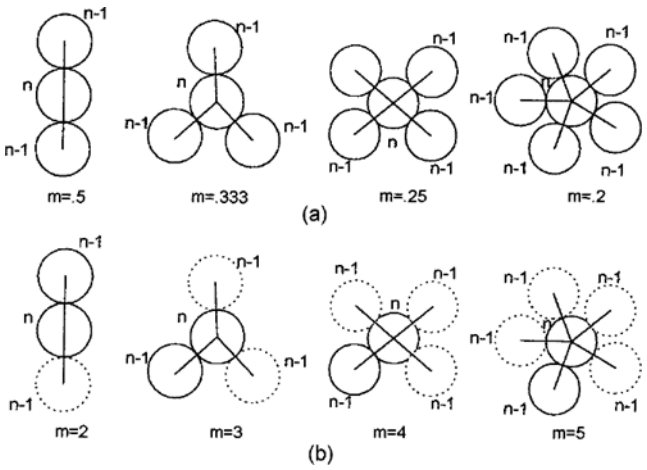

Fig. 3. Schematic cross-section views of the condensed (n−1)th layer molecules around the condensed center nth molecule to depict the negativity of the additional energy q in the nth layer of the capillary pore.

walls for a pore are assumed to participate in the adsorption. Since generally the adsorbent which has the capillary pores is composed of a single material, the adsorption sites exist in the inside and the outside of the pore. Occasionally they exist only in the inside of the pore. Then in the former the condensation adsorption occurs simultaneously in the inside and the outside of the pore first. Since only the free surface sites as shown in Fig. 2 after the pore has been filled completely adsorb the gas molecules continuously, the peculiar adsorption isotherms appear as shown in Figs. 1, 2, 3 and 7 of the literature [Prenzlow and Halsey, 1957].

The adsorbed molecules on the nth and (n−1)th layers according to the values of m are shown in Figs. 3 and 4. When the values of m are 0.5, 0.333, 0.25 and 0.2, it is easily determined that a pore has 2, 3, 4 or 5 flat adsorption walls. When the values of m are larger than unity, the molecules shown as the dotted lines represent that they are not able to be adsorbed. When m=1, one dimensional surface adsorption occurs so that the adsorbed molecules to a site can grow alternatively with both directions. Fig. 4 shows the states when the center of the condensation film is vacant. The possibility for the existence of those two cases (Figs. 3 and 4) is found in the research for the ice crystals of the cold clouds as shown in Fig. 9.14 of Salby's book [Salby, 1996]. Since the state of Fig. 4 is more mobile than that of Fig. 3, the number of the states of Fig. 4 is a little less than that of Fig. 3 in that figure. Therefore, we ignore

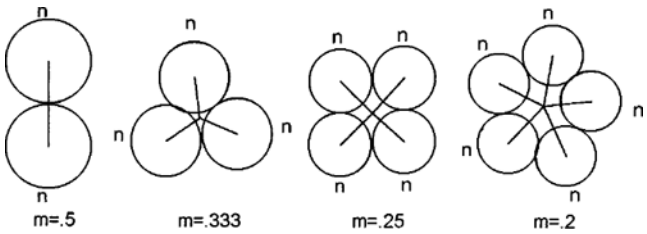

Fig. 4. Schematic cross-section views of the condensed nth layer molecules around the center potential line to depict the negativity of the additional energy q in the nth layer of the capillary pore.

considering the states of Fig. 4 in the present derivation.

There are two cases: one, the Bose-Einstein [McQuarrie, 1973] condensation adsorption occurs simultaneously both in the inside and the outside of the pore; two, it occurs only in the inside of the pore. Here Bose-Einstein condensation means that a gas molecule is adsorbed on the other gas molecule. And then an infinite number of gas molecules can be adsorbed on it. But since the size of the pore is limited in the pore condensation adsorption, only a limited number of gas molecules are adsorbed. We use Bose-Einstein condensation because it can occur characteristically if there is no pore. It seems that the pore of the adsorbent where the condensation adsorption occurs only in its inside is made when it is treated at a high temperature. The theoretical adsorption isotherms of types IV and V derived in the present study show the finishing of the horizontal beginning with respect to the x axis. The reason is that condensation adsorption does not occur any more after the pore is plugged. Then the amount of the adsorbed molecules is constant even if the relative pressure increases. But practically, the condensation adsorption increases continuously little by little until the saturation pressure is reached. This brings the flat horizontal increase in the finishing part of the isotherm.

If indistinguishable molecules, N_1/m, are adsorbed on B_1, the identical sites on the inside wall of the pore by Fermi-Dirac statistics, the complete partition function, $Q_{s1}(N_1, m, B_1, T)$, for the adsorbed molecules is determined by multiplying the configuration partition function with N_1/m square of the molecular partition as follows [Kim, 2000]:

$$Q_{s1}(N_1, B_1, m, T) = \frac{B_1!}{\left(B_1 - \frac{N_1}{m}\right)!\left(\frac{N_1}{m}\right)!}\{j_{s1}\exp(D_{s1}/kT)\}^{N_1/m} \tag{1}$$

In Eq. (1) the spatial arrangement of the sites on the adsorbent is immaterial. So we set up Eq. (1) first by considering the sites on the inside wall of the circular capillary such as the sites on the flat surface. In Eq. (1) $j_{s1}\exp(D_{s1}/kT)$ is a molecular partition function of an adsorbed molecule on the inside wall surface of the capillary pore having all degrees of freedom. In Eq. (1) j_{s1} and D_{s1} represent a local molecular partition function (including vibration and rotation partition functions) for convenience and an adsorption reaction energy. D_{s1} is larger than Bose-Einstein condensation energy, D_{l1} or D_{l2}, in the type IV isotherm and smaller than D_{l1} or D_{l2} in type V isotherm. And in Eq. (1) k and T are the Boltzmann constant and the absolute temperature of the system. Next for the multi-layer adsorption from the second to the nth layers, if the indistinguishable molecules, N_2/m, N_3/m, …, and N_n, are adsorbed on the sites, N_1/m, N_2/m, …, and N_{n-1}/m, by Fermi-Dirac statistics, the complete partition function of the adsorbed molecules from the second to nth layers becomes

$$Q_{l1}(N_1, N_2, N_3, \cdots, N_{n-1}, N_n, m, q, T) = \frac{\left(\frac{N_1}{m}\right)!\{j_{l1}\exp(D_{l1}/kT)\}^{\left(N-\frac{N_1}{m}-N_n\right)}\left\{j_{l1}\exp\left(\frac{D_{l1}+\frac{q}{m}}{kT}\right)\right\}^{N_n}}{\left(\frac{N_1}{m}-\frac{N_2}{m}\right)!\left(\frac{N_2}{m}-\frac{N_3}{m}\right)!\cdots\left(\frac{N_{n-1}}{m}-N_n\right)!N_n!}$$

$$= \frac{\left(\frac{N_1}{m}\right)!\{j_{l1}\exp(D_{l1}/kT)\}^{\left(N-\frac{N_1}{m}\right)}\{\exp(q/(mkT))\}^{N_n}}{\left(\frac{N_1}{m}-\frac{N_2}{m}\right)!\left(\frac{N_2}{m}-\frac{N_3}{m}\right)!\cdots\left(\frac{N_{n-1}}{m}-N_n\right)!N_n!} \tag{2}$$

where

$$N = \frac{1}{m}(N_1 + N_2 + \cdots + N_{n-1}) + N_n \tag{2}'$$

In Eq. (2) $j_{l1}\exp(D_{l1}/kT)$ is a molecular partition function of the molecule adsorbed on any one layer among from the second to nth layers. And in Eqs. (2) and (2)′ n represents the order number of the last adsorption layer in the polymer-like adsorption but the order number of the last adsorbed molecule in the lump-like adsorption as shown in Fig. 2. As mentioned previously, D_{l1} is the Bose-Einstein condensation energy of the adsorbed molecules from the second to nth layers. This Bose-Einstein condensation energy is smaller than the liquefaction energy of the gas molecule. It is the energy required for situating in a lower level than the free gas molecule. In Eq. (2) q/m is the additional energy of the adsorbed molecule on the nth layer with respect to 1/m walls. Hence the total macro-state partition function [Sears and Salinger, 1975] for all the adsorbed molecules over all layers at a constant temperature becomes

$$Q_M(N_1, N_2, \cdots, N_n, m, B_1, q, T) = \sum_{N_1}\cdots\sum_{N_{n-1}} Q_{s1}Q_{l1} \tag{3}$$

$\fallingdotseq$ In Eq. (3) the limit of the summation is not known and not necessary. The total adsorption energy, U, of the system becomes

$$U = \frac{D_{s1}N_1}{m} + D_{l1}\left(N - \frac{N_1}{m}\right) + \frac{N_n q}{m} \fallingdotseq u_{c1}N \tag{4}$$

In Eq. (4) u_{c1} is the average adsorption energy of an adsorbed molecule with respect to all layers. It is considered that the largest macro-state in Eq. (3) dominates the total macro-state partition function. Hence the following equation should be accomplished so that Eq. (3) has a maximum value.

$$d\ln Q_M \fallingdotseq \frac{\partial \ln Q_{s1}Q_{l1}}{\partial N_1}dN_1 + \frac{\partial \ln Q_{s1}Q_{l1}}{\partial N_2}dN_2 + \cdots + \frac{\partial Q_{s1}Q_{l1}}{\partial N_{n-1}}dN_{n-1} = 0 \tag{5}$$

If Eq. (5) is to be satisfied, the coefficient of each term should be zero. Hence by using $\partial \ln Q_{s1}Q_{l1}/\partial N_1 = 0$ we obtain

$$\frac{B_1 - N_1}{\beta_{c1}}\left\{\frac{N_n}{g\left(\frac{N_{n-1}}{m} - N_n\right)}\right\} = N_1 - N_2 \tag{6}$$

where

$$\beta_{c1} = \frac{j_{l1}}{j_{s1}}\exp\{(D_{l1} - D_{s1})/kT\} \tag{6}'$$

$$g = \exp\{q/(mkT)\} \tag{6}''$$

And by using the equations $\partial \ln Q_{s1}Q_{l1}/\partial N_2 = 0$, …, $\partial \ln Q_{s1}Q_{l1}/\partial N_{n-2} = 0$, and $\partial \ln Q_{s1}Q_{l1}/\partial N_{n-1} = 0$ we obtain

$$(N_1-N_2)\left\{\frac{N_n}{g\left(\frac{N_{n-1}}{m}-N_n\right)}\right\}=N_2-N_3$$

$$\vdots$$

$$(N_{n-3}-N_{n-2})\left\{\frac{N_n}{g\left(\frac{N_{n-1}}{m}-N_n\right)}\right\}=N_{n-2}-N_{n-1}$$

$$(N_{n-2}-N_{n-1})\left\{\frac{N_n}{g\left(\frac{N_{n-1}}{m}-N_n\right)}\right\}=N_{n-1}-mN_n \tag{7}$$

When Eqs. (3) and (4) are introduced into the combined thermodynamics 1st and 2nd law equation, Tds=dU−μdN, the chemical potential of the adsorbed molecules becomes

$$\frac{\mu_N}{kT}=\frac{u_{c1}}{kT}-\frac{\partial Q_{s1}Q_{l1}}{\partial N}=\frac{u_{c1}}{kT}-\ln\left(\frac{N_n}{m}-N_n\right)+\ln N_n-\left(\ln j_{l1}+\frac{D_{l1}}{kT}\right)-\frac{q}{mkT} \tag{8}$$

The chemical potential of the adsorbate molecules in the gas phase is generally defined as

$$\frac{\mu_G}{kT}=\frac{\mu^0}{kT}+\ln\frac{p}{p_0} \tag{9}$$

Since the adsorption is measured at the equilibrium state between the gas phase and the adsorbed phase, that is, $\mu_N=\mu_G$, by equating Eq. (8) to Eq. (9) and defining the saturation vapor pressure factor we obtain

$$c_{c1}x=c_{c1}\frac{p}{p_0}=\frac{N_n}{\frac{N_{n-1}}{m}-N_n} \tag{10}$$

where

$$c_{c1}=\frac{N_{ns}}{\frac{N_{n-1s}}{m}-N_{ns}} \tag{10}'$$

In Eq. (10)' N_{n-1s} and N_{ns} are the numbers of the molecules adsorbed on the (n−1)th and nth layers at the saturation vapor pressure. After we have multiplied Eqs. (6) and (7) side by side, by introducing Eq. (10) into the resulting equation and rearranging we obtain the number of adsorbed molecules on the nth layer as follows:

$$N_n=\left(\frac{1}{m}\right)\left(\frac{mB_1-N_1}{\beta_{c1}}\right)z^n g \tag{11}$$

where

$$z=\frac{c_{c1}x}{g} \tag{11}'$$

After we have added Eqs. (6) and (7) side by side, by introducing Eq. (10) into the resulting equation we obtain

$$N_1=\frac{mB_1\left(\frac{z-z^n}{1-z}+gz^n\right)}{\beta_{c1}+\left(\frac{z-z^n}{1-z}+gz^n\right)} \tag{12}$$

Eq. (12) is the same type of surface mono-layer adsorption isotherm as that obtained from the BET equation with n layers. But x of the latter is changed into z. Finally by combining Eqs. (6), (7), (10), (11), (11)' and (12) the capillary condensation adsorption isotherm on the porous adsorbent composed of 1 group of sites is obtained as follows

$$\frac{N}{B_1}=\frac{\frac{1}{m}(N_1+N_2+\cdots+N_{n-1})+N_n}{B_1}$$

$$=\frac{(N_1-N_2)+2(N_2-N_3)+\cdots+(n-1)(N_{n-1}-N_n)+(n-1)N_n+mN_n}{mB_1}$$

$$=\frac{\left\{\frac{z-z^n}{(1-z)^2}-\frac{(n-1)z^n}{(1-z)}+\frac{(n-1)+m}{m}gz^n\right\}}{\left(\beta_{c1}+\frac{z-z^n}{1-z}+z^n g\right)} \tag{13}$$

Eq. (13) is a linear function of z with the unknown variables m, n and β_{c1}. Since q=0 and m=1 for the adsorption on the non-porous adsorbent, it becomes the BET equation with n layers.

2. Capillary Condensation Adsorption Isotherm for the Gas Molecules Adsorbed on the Porous Adsorbent Composed of Two Groups of Sites

Let us suppose that gas molecules are adsorbed on the porous adsorbent composed of two groups of sites as shown in Fig. 2. If the indistinguishable molecules, N_{11}/m and N_{12}/m, N_{21}/m and N_{22}/m, …, N_{n1} and N_{n2} are independently adsorbed on the sites, B_1 and B_2, N_{11}/m and N_{12}/m, …, N_{n-11}/m and N_{n-12}/m, and the adsorption proportional constant M between groups is assumed as follows,

$$M=\frac{N_{12}}{N_{11}}=\frac{N_{22}}{N_{21}}=\cdots=\frac{N_{n2}}{N_{n1}} \tag{14}$$

the complete partition functions of the adsorbed molecules in the 1st layer become for group 1

$$Q_{s1}=\frac{B_1!}{\left(B_1-\frac{N_{11}}{m}\right)!\left(\frac{N_{11}}{m}\right)!}\{j_{s1}\exp(D_{s1}/kT)\}^{N_{11}/m} \tag{15}$$

for group 2

$$Q_{s2}=\frac{B_2!}{\left(B_2-\frac{MN_{11}}{m}\right)!\left(\frac{MN_{11}}{m}\right)!}\{j_{s2}\exp(D_{s2}/kT)\}^{MN_{11}/m} \tag{16}$$

In Eqs. (15) and (16) $j_{s1}\exp(D_{s1}/kT)$ and $j_{s2}\exp(D_{s2}/kT)$ are the molecular partition functions of the molecules adsorbed in the first layer of groups 1 and 2. And the complete partition functions of the adsorbed molecules on the sites of groups 1 and 2 from the 2nd to nth layer become independently

$$Q_{t1}=\frac{\left(\frac{N_{11}}{m}\right)!\{j_{t1}\exp(D_{t1}/kT)\}^{\left(\frac{N}{1+M}-\frac{N_{11}}{m}\right)}\{\exp(q/(mkT))\}^{N_{n1}}}{\left(\frac{N_{11}}{m}-\frac{N_{21}}{m}\right)!\left(\frac{N_{21}}{m}-\frac{N_{31}}{m}\right)!\cdots\left(\frac{N_{n-11}}{m}-N_{n1}\right)!N_{n1}!} \quad (17)$$

$$Q_{t2}=\frac{\left(\frac{MN_{11}}{m}\right)!\{j_{t2}\exp(D_{t2}/kT)\}^{\left(\frac{MN}{1+M}-\frac{MN_{11}}{m}\right)}\{\exp(q/(mkT))\}^{MN_{n1}}}{\left\{\frac{M}{m}(N_{11}-N_{21})\right\}!\left\{\frac{M}{m}(N_{21}-N_{31})\right\}!\cdots\left(\frac{MN_{n-11}}{m}-MN_{n1}\right)!(MN_{n1})!} \quad (18)$$

Where

$$N=(1+M)\left(\frac{N_{11}+N_{21}+\cdots+N_{n-11}}{m}+N_{n1}\right) \quad (19)$$

In Eqs. (17) and (18) $j_{t1}\exp(D_{t1}/kT)$ and $j_{t2}\exp(D_{t2}/kT)$ are the molecular partition functions of groups 1 and 2 for the adsorbed molecules on the sites from the 2nd to nth layer. As done in the above section the total adsorption energy U of the system for all the adsorbed molecules on the porous adsorbent becomes

$$U=\frac{D_{s1}N_{11}}{m}+\frac{D_{s2}MN_{11}}{m}+D_{t1}\left(\frac{N}{1+M}-\frac{N_{11}}{m}\right)+\frac{(1+M)N_{n1}q}{m}+D_{t2}\left(\frac{MN}{1+M}-\frac{MN_{11}}{m}\right)\fallingdotseq u_{c2}N \quad (20)$$

In Eq. (20) u_{c2} is the average adsorption energy of an adsorbed molecule with respect to all groups and layers. Hence the total macro-state partition function for all the adsorbed molecules over all layers at a constant temperature becomes

$$Q_{t5}(N_{11},N_{21},\cdots,N_{n1},m,M,B_1,B_2,q,T)=\sum_{N_{11}}\cdots\sum_{N_{n-1n}}Q_{s1}Q_{s2}Q_{t1}Q_{t2} \quad (21)$$

In Eq. (21) the limit of the summation is not known and not needed. It is considered that the largest macro-state in Eq. (21) dominates the total macro-state partition function. Hence the following equation should be accomplished so that Eq. (21) has a maximum value.

$$d\ln Q_{t5}\fallingdotseq\frac{\partial\ln Q_{t5}}{\partial N_{11}}dN_{11}+\frac{\partial\ln Q_{t5}}{\partial N_{21}}dN_{21}+\cdots+\frac{\partial Q_{t5}}{\partial N_{n-11}}dN_{n-11}=0 \quad (22)$$

where

$$Q_{t5}=Q_{s1}Q_{s2}Q_{t1}Q_{t2} \quad (22)'$$

If Eq. (22) is to be satisfied, the coefficient of each term should be zero. Hence by using $\frac{\partial\ln Q_{s1}Q_{s2}Q_{t1}Q_{t2}}{\partial N_{11}}=0$ we obtain

$$\left\{\frac{(mB_1-N_{11})(mB_2-MN_{11})^M}{M^M\beta_{c2}}\right\}^{\frac{1}{1+M}}\left\{\frac{1}{g}\left(\frac{N_{n1}}{\frac{N_{n-11}}{m}-N_{n1}}\right)\right\}=N_{11}-N_{21} \quad (23)$$

where

$$\beta_{c2}=\left(\frac{j_{t1}}{j_{s1}}\right)\left(\frac{j_{t2}}{j_{s2}}\right)^M\exp\left[\{(D_{t1}-D_{s1})+M(D_{t2}-D_{s2})\}/kT\right] \quad (23)'$$

$$g=\exp[q/(mkT)] \quad (6)''$$

And by using the remaining coefficient equations, $\partial\ln Q_t/\partial N_{21}=0$, …, $\partial\ln Q_t/\partial N_{n-11}=0$, and $\partial\ln Q_t/\partial N_{n-11}=0$, we obtain

$$(N_{11}-N_{21})\left\{\frac{1}{g}\left(\frac{N_{n1}}{\frac{N_{n-1}}{m}-N_{n1}}\right)\right\}=N_{21}-N_{31}$$

$$\vdots$$

$$(N_{n-31}-N_{n-21})\left\{\frac{1}{g}\left(\frac{N_{n1}}{\frac{N_{n-11}}{m}-N_{n1}}\right)\right\}=N_{n-21}-N_{n-11}$$

$$(N_{n-2}-N_{n-11})\left\{\frac{1}{g}\left(\frac{N_{n1}}{\frac{N_{n-11}}{m}-N_{n1}}\right)\right\}=N_{n-11}-mN_{n1} \quad (24)$$

As done for the chemical potential in section 2 we obtain the following equation:

$$c_{c2}x=c_{c2}\frac{p}{p_0}=\frac{N_{n1}}{\frac{N_{n-11}}{m}-N_{n1}} \quad (25)$$

where

$$c_{c2}=\frac{N_{n1s}}{\frac{N_{n-11s}}{m}-N_{n1s}} \quad (25)'$$

In Eq. (25)' the subscript s indicates that the adsorption data are measured at the saturation vapor pressure. In Eqs. (23) and (24) after we have multiplied all the equations side by side, by introducing Eq. (25) into the resulting equation we obtain

$$N_{n1}=\frac{1}{m}\left\{\frac{(mB_1-N_{11})(mB_2-MN_{11})^M}{M^M\beta_{c2}}\right\}^{\frac{1}{1+M}}z^ng \quad (26)$$

$$z=\frac{c_{c2}x}{g} \quad (26)$$

In Eqs. (23) and (24) after we have added all the equations side by side, by introducing Eq. (25) into the resulting equation we obtain

$$N_{11}=\left\{\frac{(mB_1-N_{11})(mB_2-MN_{11})^M}{M^M\beta_{c2}}\right\}^{\frac{1}{1+M}}\left(\frac{z-z^n}{1-z}+gz^n\right) \quad (27)$$

Therefore by combining Eqs. (25), (26) and (27) the capillary condensation adsorption isotherm for the gas molecules adsorbed on the porous adsorbent composed of the sites of 2 groups is obtained as follows:

$$\frac{N}{B_1+B_2}=\frac{\frac{1}{m}\{N_{11}+N_{21}+\cdots+N_{n-11}+M(N_{11}+N_{21}+\ldots+N_{n-11})\}+N_{n1}+MN_{n1}}{(B_1+B_2)}$$

$$=\frac{a_1}{m}\left\{\frac{(mB_1-N_{11})(mB_2-MN_{11})^M}{M^M\beta_{c2}}\right\}^{\frac{1}{1+M}}$$

$$\left\{\frac{z-z^n}{(1-z)^2}-\frac{(n-1)z^n}{1-z}+\frac{(n-1+m)}{m}gz^n\right\} \tag{28}$$

where

$$a_1=\frac{1+M}{(B_1+B_2)} \tag{28'}$$

In Eq. (28) N_{11} is obtained from Eq. (27). It is a nonlinear function of z with the unknown variables, m, M, and β_{c2}, and can be solved numerically. When $B_1=B_2$, $j_{s1}=j_{s2}$, $j_{l1}=j_{l2}$, $D_{s1}=D_{s2}$, $D_{l1}=D_{l2}$, and M=1 of Eq. (28) for one group of sites, it becomes Eq. (13). And when m=1 and q=0 of Eq. (28) for the non-porous adsorbent, Eq. (28) becomes the adsorption isotherm with n layers composed of two groups of sites.

3. Surface Mono-layer Adsorption Isotherms in the Non-porous and the Porous Adsorbents

Point B in the BET type isotherms is the point at which the isotherm indicates the completion of the adsorption of the surface sites. The adsorption amount at point B is called x_B. Generally, point B is read as the beginning point of the linear portion of the adsorption isotherm of type II or IV. In the previous literature [Kim, 2000] we mentioned mostly the simultaneity of the Fermi-Dirac adsorption and Bose-Einstein condensation adsorption in differential heat parts. After the sites of the first layer have been occupied completely by the adsorbate molecules, we do not think that the higher than 2nd layers are adsorbed. We discuss this in the surface monolayer adsorption isotherms which was already derived in the literature [Kim, 2000; Hill, 1946a] and in the above sections.

Eq. (25) of Hill's literature [Hill, 1946a] being rearranged, the surface mono-layer adsorption isotherm for the BET equation with n limited number of layers obtained for the adsorbed gas molecules in the non-porous adsorbent becomes

$$\frac{N_1}{B_1}=\frac{\dfrac{x-x^n}{1-x}+x^n}{\beta+\dfrac{x-x^n}{1-x}+x^n} \tag{29}$$

Hence the surface monolayer adsorption isotherm for the BET equation with infinite number of layers becomes as follows because $x^n\rightarrow 0$ for $n\rightarrow\infty$.

$$\frac{N_1}{B_1}=\frac{x}{\beta(1-x)+x} \tag{30}$$

Eq. (30) is the same type as the Langmuir isotherm [Langmuir, 1918].

The surface mono-layer adsorption isotherm for the infinite adsorbed molecules on the non-porous adsorbent composed of two groups of sites is obtained by combining Eq. (15) with the θ value in Eq. (16) in the previous literature [Kim, 2000] as follows:

$$\frac{(1+M_1)N_{11}}{B_1+B_2}=(1-c_{s1}x)\theta \tag{31}$$

The surface mono-layer adsorption isotherm with n limited number of layers for the non-porous adsorbent is obtained by rearranging Eq. (29) in our previous literature [Kim, 2000] as follows:

$$\frac{(1+M)N_{11}}{B_1+B_2}=a_1\left\{\frac{(B_1-N_{11})(B_2-M_1N_{11})^{M_1}}{M_1^{M_1}\beta_2}\right\}^{\frac{1}{1+M_1}}\left\{\frac{c_{s2}x-(c_{s2}x)^{n+1}}{1-c_{s2}x}\right\} \tag{32}$$

Eq. (32) becomes Eq. (31) when $n\rightarrow\infty$ (ca. n>50).

From Eq. (12) we get for the surface mono-layer adsorption isotherm of the porous adsorbent composed of one group of sites

$$\frac{N_1}{mB_1}=\frac{\dfrac{z-z^n}{1-z}+gz^n}{\beta_{c1}+\dfrac{z-z^n}{1-z}+gz^n} \tag{33}$$

and from Eq. (27) we get for the surface mono-layer adsorption isotherm of the porous adsorbent composed of two groups of sites

$$\frac{N_{11}(1+M)}{m(B_1+B_2)}=\frac{a_1}{m}\left\{\frac{(mB_1-N_{11})(mB_2-MN_{11})^M}{M^M\beta_{c2}}\right\}^{\frac{1}{1+M}}\left(\frac{z-z^n}{1-z}+gz^n\right) \tag{34}$$

RESULTS AND DISCUSSION

1. Condensation Adsorption Isotherms for the Adsorbed Molecules on the Porous Adsorbents Composed of One or Two Groups of Sites

As shown in Fig. 5, the type IV adsorption isotherm shows the same type of adsorption as the BET isotherm at a lower relative vapor pressure, but it finishes with the beginning of horizontality near the saturated vapor pressure. Numerically, we can read that fact exactly, but the figure does not depict it clearly. The cause originates from ignoring to consider the continuous adsorption after the pore has been filled naturally by statistics. We also ignored the adsorption on the outside sites of the pore. Hence Fig. 5 becomes the adsorption isotherm which finishes pore condensation near x=1. It is possible when q is negative for the adsorption to be finished with the beginning of the horizontality. That illustrates the agreement of the isotherm with the experimental data. Fig. 6 shows the

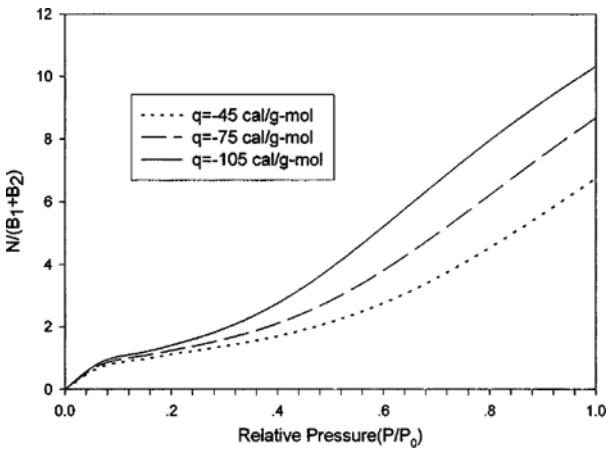

Fig. 5. Theoretical capillary condensation adsorption isotherms Eq. (28) (β_{c2}=.00179, T=20 °C, M=1, m=.23, B_1=25, B_2=25, c_{s2}=.76, n=7) vs. various q (additional energy) values.

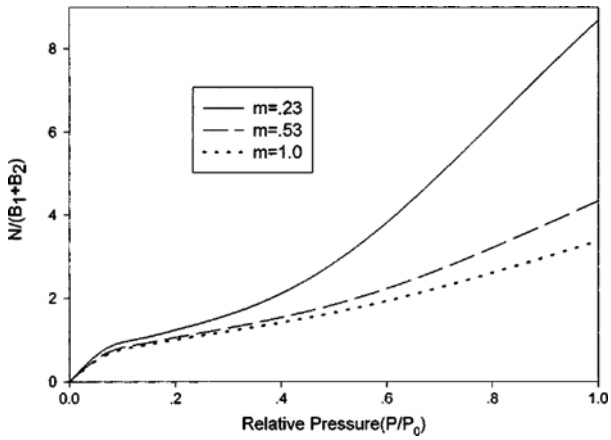

Fig. 6. Theoretical capillary condensation adsorption isotherms Eq. (28) (β_{c2}=.00179, T=20 °C, q=−75 cal/g-mol, M=1, B_1=25, B_2=25, c_{c2}=.76, n=7) vs. various 1/m (no. of parallel walls) values.

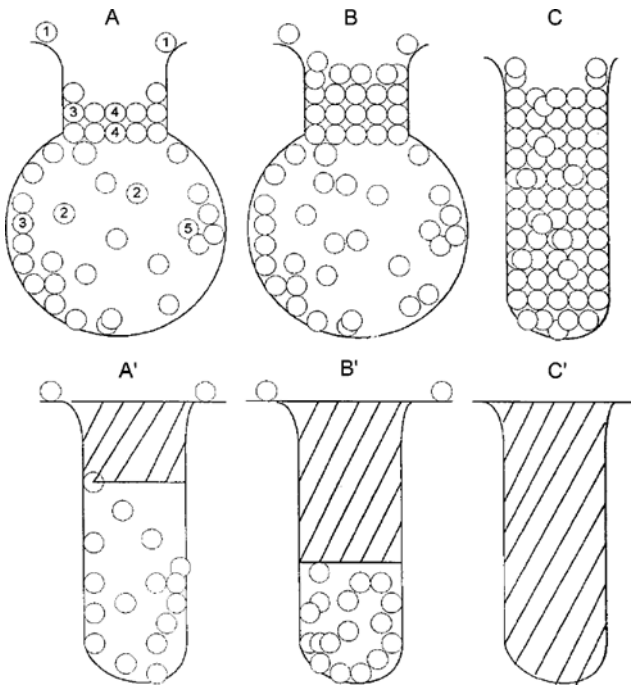

Fig. 7. Schematic representation of type IV adsorption in ink bottle-type pores and their cylinderical capillary pores. Blank circles represents adsorbed molecules and a solid lined part represents the condensation of the adsorbed molecules.

capillary condensation adsorption isotherms according to m values.

When β_{c1} of Eq. (13) or β_{c2} of Eq. (28) is less than unity, the adsorption isotherm shows type IV. The models shown in Fig. 7 depict the adsorbed molecules in the ink bottle and in the capillary. The contact angle of the meniscus of the condensate film is larger than 0° and smaller than 90°. The contact angle generally depends on the harmony between the surface tension of the adsorbed molecules and the adhesion force with the wall of the capillary. It is considered that adsorbate like Hg vapor makes a much different contact angle with the capillary wall from general gases in Type IV.

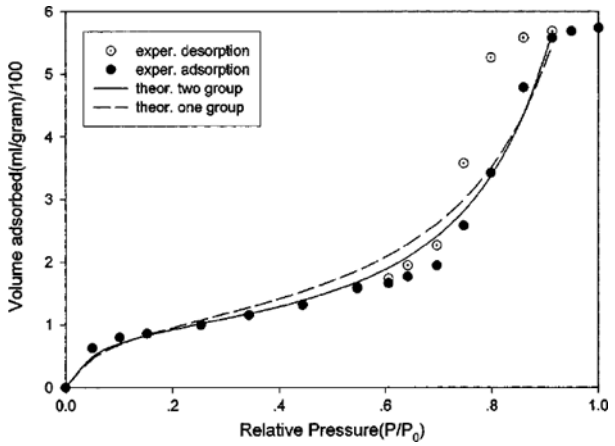

Fig. 8. Theoretical capillary isotherm of one group sites Eq. (13) (β_{c1}=.0611, q=−39.9 cal/g-mol, m=50, n=25, c_{c1}=.50) and two group sites Eq. (28) (β_{c2}=.00092, q=−64.3 cal/g-mol, M=1.4, m=86, B_1=25, B_2=50, c_{c2}=.59, n=26) compared with the experimental nitrogen adsorption isotherm data on silica at 78 K [Shull, 1948].

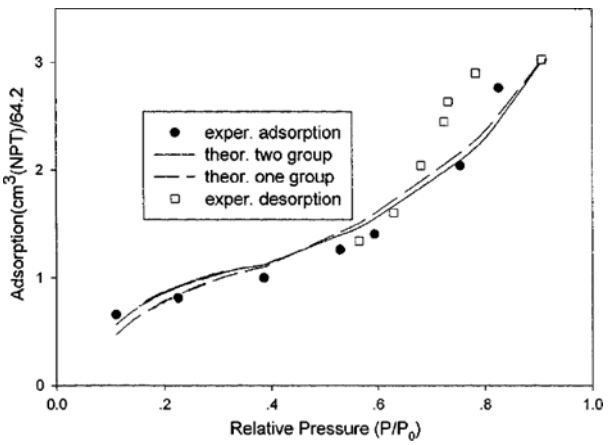

Fig. 9. Theoretical capillary condensation adsorption isotherm (type IV) of one group sites Eq. (13) (β_{c1}=.1211, q=−35 cal/g-mol, m=.62, n=15, c_{c1}=.53) and two group sites Eq. (28) (β_{c2}=.003, q=−47.5 cal/g-mol, M=1.4, m=.65, B_1=25, B_2=50, c_{c2}=.51, n=17) compared with the experimental adsorption-desorption isotherm of nitrogen adsorbed on titania at 78 K [Harris and Whitaker, 1963].

The isotherms of type IV selected among a number of the experimental adsorption-desorption isotherms are shown in Figs. 8-10. Shull [Shull, 1948] conducted an experiment about the adsorption-desorption of nitrogen on silica gel at 78 K (Fig. 8), Harris and Whitaker [Harris and Whitaker, 1963] the adsorpton-desorption of nitrogen on Titania at 78 K (Fig. 9), and Emmett and Cines [Emmett and Cines, 1947] the adsorption-desorption of water on the porous glass at 26.5 °C (Fig. 10). As we see in the figures, the condensation adsorption isotherm of Eq. (13) of one group of sites agrees with the experimental data a little less than does the condensation adsorption isotherm of Eq. (28) of two groups of sites. As mentioned in the previous literature [Kim, 2000], we discussed that all the non-porous adsorbents had two groups of sites. These non-porous adsorbents can be made into the porous adsorbents of

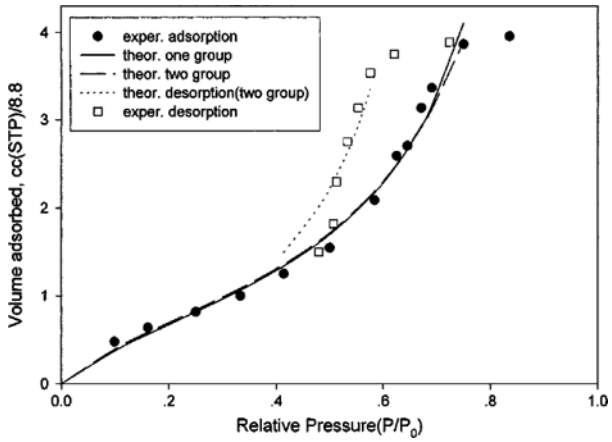

Fig. 10. Theoretical capillary condensation adsorption isotherm (type IV) of one group sites Eq. (13) (β_{c1}=.2091, q=−93 cal/g-mol, m=.3, c_{c1}=.61, n=15) and two sites Eq. (28) (β_{c2}=.0240, q=−92.2 cal/g-mol, M=1.57, m=.3, B_1=25, B_2=50, c_{c2}=.63, n=15) compared with the experimental adsorption-desorption isotherm of water adsorbed on porous glass No. 7 at 26.5 °C [Emmett and Cines, 1947].

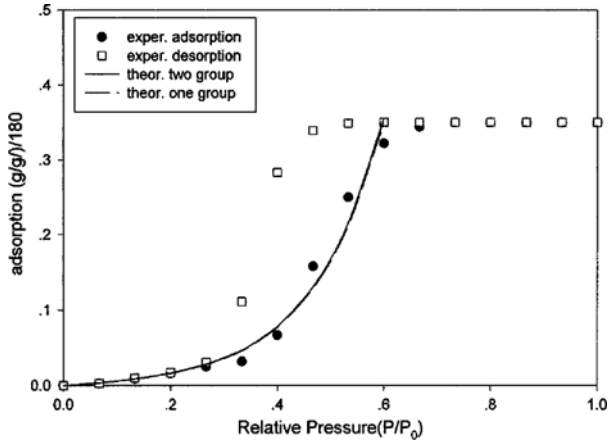

Fig. 12. Theoretical capillary condensation isotherms (type V) of one group sites Eq. (13) (β_{c1}=30.21, q=−75 cal/g-mol, m=.23, n=7, c_{c1}=.76) and two groups sites Eq. (28) (β_{c2}=912.59, q=−75.0 cal/g-mol, M=1.0, m=.23, B_1=25, B_2=25, c_{c2}=.75, n=7) compared with experimental adsorption-desorption isotherm of water vapor adsorbed on activated polyvinyl chloride carbon (58.8%) at 20 °C [Kipling and Wilson, 1960].

type IV. So it is believed that the adsorbents used in Figs. 8, 9 and 10 have two groups of sites.

When β_{c1} of Eq. (13) or β_{c2} of Eq. (28) is larger than unity, type V isotherm is obtained. We show the models of the schematic adsorbed molecules in the ink bottle and in the capillary in Fig. 11. Their isotherms belong to type V. The contact angle of the meniscus becomes larger than 270° and smaller than 360°. Not many experimental data exist for the adsorption-desorption of type V. Kipling and Wilson's experiment for the adsorption-desorption of H_2O on polyvinyl chloride carbon (58.8%) at 20 °C (Fig. 12) [Kipling and Wilson, 1960] and Wig and Juhola's experiment for the adsorption-desorption of H_2O on charcoal (N-19) at 24 °C (Fig. 13) [Wig and Juhola, 1949] are discussed. As shown in Fig. 12 and 13, Eqs. (13) and (28) agree with the experimental data almost similarly. It may be because the wall of the porous adsorbent is composed of the sites of one group. But we think that the porous adsorbents of type V are composed of two groups of sites. Type V isotherms generally show a small amount of adsorption in the be-

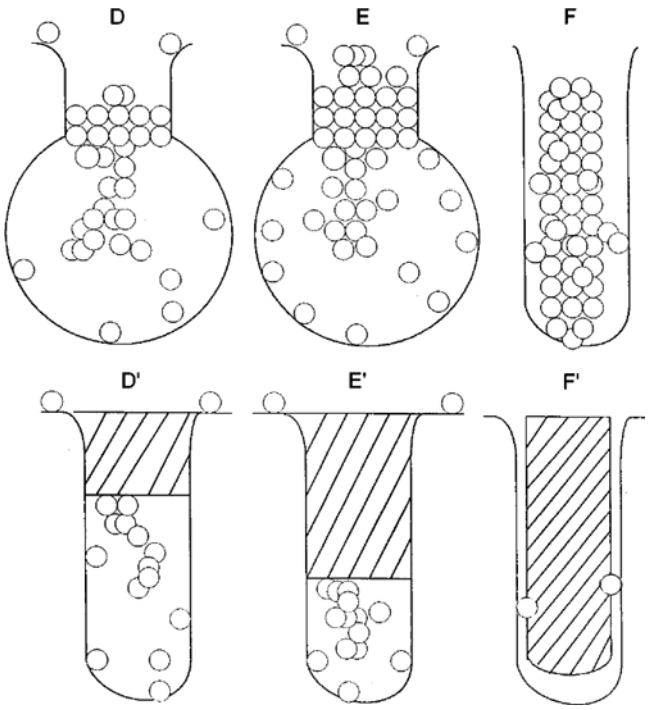

Fig. 11. Schematic representation of type V adsorption in ink bottle-type pores and their cylinderical capillary pores. Blank circles represents adsorbed molecules and a solid lined part represents the condensation of the adsorbed molecules.

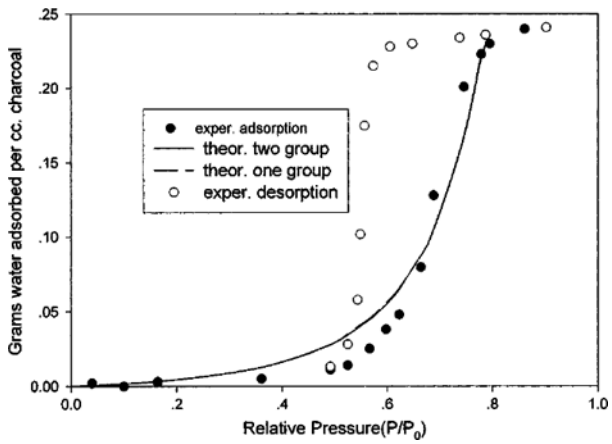

Fig. 13. Theoretical capillary condensation adsorption isotherms (type V) of one group sites Eq. (13) (β_{c1}=73.98, q=−98.5 cal/g-mol, m=.31, n=14, c_{c1}=.6) and two groups sites Eq. (28) (β_{c2}=5473.2, q=−98.0 cal/g-mol, M=1.0, m=.31, B_1=24, B_2=24, c_{c2}=.6, n=14) compared with the experimental adsorption-desorption isotherm of water adsorbed on charcoal N-19 at 24 °C [Wig and Juhola, 1949].

Table 1. Monolayers, surface areas, pore radii, etc. obtained from capillary condensation adsorption isotherms of Eq. (13) (one group) and Eq. (28) (two group) for various experimental data

Adsorbent (type)	Adsorbate (Temper.)	v_m through Eq. (39) (group or BET)	S_N or S_W (m^2/g)	Number of layers (n)	Thickness of a molecule (σ, Å)	nσ (pore radius; k_c, Å)
Silica	N_2 (78 K)	96.26 ml/g (1)	416.6	25	3.5	88
(IV)		99.02 ml/g (2)	428.6	26	3.5	91(90[a])
[Shull, 1948]		39.5 ml/g (BET)	170.9			
Titania	N_2 (78 K)	65.6 cm^3/g (1)	284.0	15	3.5	54
(IV)		56.0 cm^3/g (2)	276.1 (186[a])	17	3.5	60(34[a])
[Harris et al., 1963]		15.3 cm^3/g (BET)	66.1			
Porous glass	H_2O (26.5 °C)	9.36 cc/g (1)	26.4	15	2.8	42
No. 7 (IV)		9.11 cc/g (2)	25.7 (128[a])	15	2.8	42 (25.9[a])
[Emmett et al., 1947]		7.16 cc/g (BET)	20.2			
Activated	H_2O (20 °C)	.964 g/g (1)	3389	7	2.8	19.6
polyvinyl ...		.951 g/g (2)	3344 (880[a])	7	2.8	19.6 (20.2[a])
(58.8 %) (V)		−.044 (BET)				
[Kippling et al., 1960]						
Charcoal	H_2O (24 °C)	.976 g/g (1)	3432	14	2.8	39.2
N-19 (V)		.975 g/g (2)	3429	14	2.8	39.2
[Wig et al., 1949]		−.0651 (BET)				

The superscript "a" means that the values are in their corresponding papers.

ginning of the relative vapor pressure. Hence, to discern two groups of sites did not role on the adsorption sufficiently. And on the other hand, the values of n in Table 1 are 7 and 14. They are not the infinitive values so that it is meaningless to discern two groups of sites. But it is considered that they role like the infinitive value.

Fig. 14 is the experimental isotherm by Barrer and Maclead which shows the hysteresis phenomena for the adsorption-desorption of nitrogen on the natural Na-rich montmorillonite at 78 K [Barrer and Maclead, 1954]. The isotherm finishes like the BET equation near x=1 . When we introduced the values of q=0, m=1 and n=∞ into Eq. (28), we couldn't fit the experimental data to it. When we used Eq. (16) in our previous literature [Kim, 2000], the fitting was reasonable as shown in Fig. 14. It is considered that the parameter values used in Fig. 14 are possible. The authors observed that a meniscus was formed in the space between two parallel plates which were not rigidly held together when the system reached the relative saturation vapor pressure. We think that if the meniscus is formed, the surface tension of the meniscus can't be ignored. So the adsorption isotherm should show the beginning of horizontality near x=1, but it is not so. Therefore, it is considered that condensation adsorption occurs on the free surface and it is believed that the gas molecules are adsorbed very lightly on the lump of the molecules adsorbed on sites because the adsorption energy is small near x=1. Hence the adsorption and desorption isotherms have the regular type II figures.

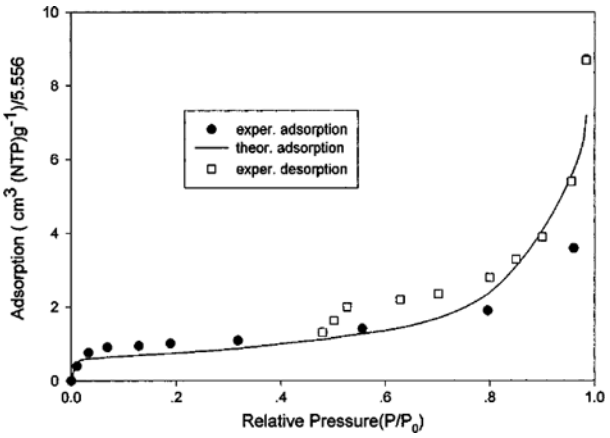

Fig. 14. Theoretical plane condensation adsorption isotherms (type II) of two group sites Eq. (16) [Kim, 2000] (β_{c1}= .00072, f_1=1.229, M_1=.360, c_{s1}=.93) compared with experimental adsorption-desorption isotherms of nitrogen adsorbed on a natural sodium-rich montmorillonite at 78 °C [Barrer and Macleod, 1964].

The values of the parameter, q, used in the above five experimental figures are considered to be reasonable because they are less than 100 cal/g-mol and much less than the Bose-Einstein condensation energy (D_{l1} or D_{l2}) used in explaining the differential heat in the previous literature [Kim, 2000]. The surface adsorption energy (D_{s1} or D_{s2}) of the adsorbents which describes type V adsorption isotherms is not known, but it is believed to be slightly less than Bose-Einstein condensation energy. We think that the surface adsorption energy, D_{s1} (or D_{s2}), may exchange D_m in Table 3 in the previous literature [Kim, 2000]. Therefore β_{c1} or β_{c2} can be larger than unity and then a type V isotherm can be obtained. Notwithstanding D_{s1} or D_{s2}>D_{l1} or D_{l2}, the reason why the pore condensation occurs is owing to the harmonized combination of the increasing of the surface adsorption (adhesive energy) and growing of the lump of H_2O by hydrogen bonding (cohesive energy). Hence, the value of q is much less than the free condensation energy (ca. 10,000 cal/g-mol at 25 °C for H_2O). The force balance of the condensation adsorption film seems to be accomplished.

The values of the parameter, m, used in the above five experimental figures seem to represent the expected values. When we

Table 2. Pore radii calculated by Kelvin equation according to relative pressures and the contact angles

Fig. 12 [Kipling et al., 1960]	$x(p/p_0)$	pore radii (Å) contact angle			Fig. 13 [Wig et al., 1949]	$x(p/p_0)$	pore radii (Å) contact angle		
		cos θ=1	cos θ=.65	cos θ=.28			cos θ=1	cos θ=.65	cos θ=.28
polyvinyl	0.4	11.70	7.61	3.28	charcoal	0.6	20.7	13.5	5.8
chloride	0.5	15.47	10.06	4.33	N-19	0.7	29.7	19.3	8.3
carbon (58.8%)	0.6	20.99	13.65	5.88		0.8	47.4	30.8	13.2

used values of m larger than unity, we couldn't fit the experimental data to the isotherm Eqs. (13) and (28) because a large standard error appeared. The values of the parameter m, used in Figs. 8-10 and Figs. 12-13 are not optimized values, but since they are the best fitted values by a number of trial and error methods, they do not create any problems by being analyzed as above. Hence the dead adsorption walls explained in Fig. 3 do not exist in Figs. 8, 9, 10, 12, 13.

The numbers of surface sites ($\fallingdotseq v_m$: the mono-layer adsorption capacity) of the adsorbents through the above used experimental data were obtained by using Eq. (13) for one group of sites and Eq. (28) for two groups of sites with the method [Eq. (39)] mentioned in the previous literature [Kim, 2000]. When we fitted the experimental data to the BET equation to get the surface mono-layer sites (v_m), we followed the same approach as above. Then the surface areas of the adsorbents according to v_m could be obtained. As we see the results in Table 1, v_ms obtained by Eq. (13) and Eq. (28) are much larger than those obtained by the BET equation. v_ms for type V couldn't be obtained through the BET equation. They gave negative values.

The pore radii (nσ) shown in Table are obtained by multiplying the number of adsorption layers (n) by the thickness (σ) of an adsorbed single molecule. → We got the pore radius of polyvinyl chloride carbon (58.8%), 19.6 Å and that of charcoal N-19, 39.2 Å by multiplying the number of adsorption layers (n=7 and 14) by the thickness (σ=2.8 Å) of an adsorbed molecule (H_2O). They agree quite well with the values obtained by the Kelvin equation [Kipling and Wilson, 1960] as showed in Table 2. It is then considered that the contact angle of the gas molecules of the pore film with the pore walls may be 270-360° and the relative vapor pressure, x, may be the beginning value of the sudden increasing part of the pore condensation adsorption isotherm. On the other hand, the x value of the inflection point of type V isotherm seems to give better agreement with the cosine value of the contact angle.

2. The Surface Mono-layer Adsorption Isotherm in Non-porous and Porous Adsorbents

Until now the isotherm equations which represent the amounts of the adsorbed mono-layer molecules have not been studied much except for the Langmuir equation. As mentioned in section 3, we can get them easily in the present study. According to them the surface layers are not adsorbed completely for the both types IV and V even when x=1 (Figs. 15, 16, 17). We can account for the error by comparing the theoretical surface mono-layer isotherms [Eqs. (29), (30), (31), (32)] with their corresponding experimental v_ms. As Figs. 15 and 16 show, one of the influential factors in the adsorption of the surface mono-layer is also the value of β_{c1} or β_{c2}, the ratio of the molecular partition functions between the surface

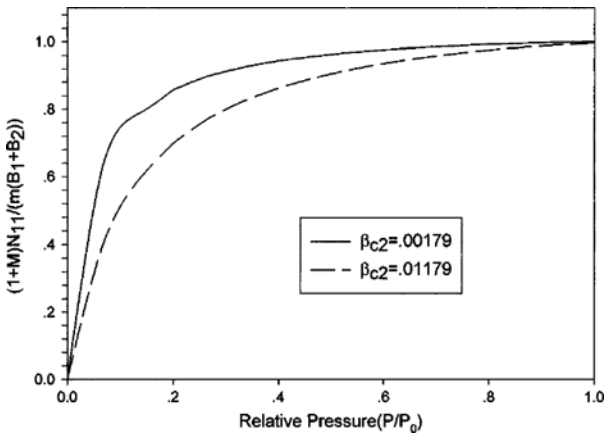

Fig. 15. Theoretical first (surface) layer adsorption isotherm Eq. (34) of capillary condensation (type IV) (q=−75 cal/g-mol, M=1, m=.23, B_1=25, B_2=25, c_{c2}=1.0, n=17, T=20 °C).

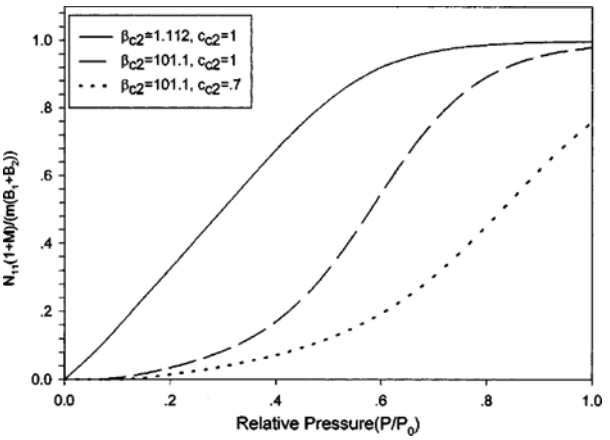

Fig. 16. Theoretical first (surface) layer adsorption isotherm (type V) of the capillary condensation Eq. (34) (q=−75 cal/g-mol, M=1, m=.23, B_1=25, B_2=25, n=10, T=20 °C).

mono-layer and the multi-layers. When β_{c1} or β_{c2} is less than unity, a type I isotherm is obtained. If the surface adsorption force, D_{s1} or D_{s2}, is much larger than D_{l1} or D_{l2}, that is, β_{c1} or β_{c2} is much smaller than unity, almost all the surface sites are occupied by gas molecules even at a low relative vapor pressure (Fig. 15). If, conversely, β_{c1} or β_{c2} is larger than unity, type V isotherm is obtained (Fig. 16) and even at the higher relative vapor pressure the many surface sites are unoccupied as shown in Fig. 17.

3. Hysteresis Phenomenon in Adsorption-desorption Isotherms of Gas Molecules

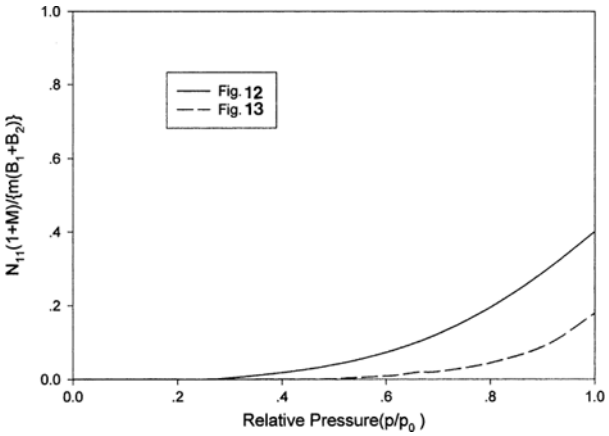

Fig. 17. Theoretical surface mono-layer adsorption isotherms (type V) of Eq. (34) using the parameters of Figs. 12 and 13.

Many researches did explain the hysteresis phenomenon of adsorption-desorption isotherms by depicting the adsorption-desorption in the ink-bottle and in the capillary pore [Gregg and Sing, 1969; Rao, 1941; Katz, 1949]. Recently, the hysteresis in the isotherms for the adsorbed molecules on the porous adsorbent was explained by the inter-connectivity of the pores [Mason, 1988]. And more than a half-century ago the Kelvin equation, $p=p_0\exp(-\gamma V/RT)$, was used to explain the hysteresis phenomenon. It is possible to apply the Kelvin equation to the experimental data in which capillary condensation occurs. But the aforementioned models do not seem to explain the characteristics of the hysteresis phenomenon concerning adsorption-desorption. While we did the present research, we learned that the hysteresis phenomenon of the adsorption-desorption isotherms for the molecules adsorbed on adsorbents originates from a deviation from the thermo-dynamically reversible process between the adsorption and the desorption of the adsorbates on the adsorbent. This phenomenon seems to apply to electro-magnetization. Recently a great deal of research on the hysteresis of electro-magnetization has been done, but a study on its cause is rare.

Thermodynamic reversibility in adsorption-desorption isotherms of the adsorbed gas molecules on the adsorbent means that at a determined relative vapor pressure the elimination history of the adsorption coincides oppositely with the supplying history of the desorption. Thermodynamic reversibility in the adsorption-desorption isotherms is rooted in bringing the maximum amount of adsorption and desorption. It is different from the explanation which Brunauer says is to be reproducible of the isotherms.

Generally, except for using a precise temperature controller, it is impossible to accomplish a thermodynamically reversible process between adsorption and desorption in a common fluid (air, water, liquefied nitrogen, etc.). When the gas molecules are adsorbed on the adsorbent, their adsorption heats are eliminated easily to get thermal equilibrium. But their desorption heats are not supplied at all when they are desorbed. The common fluid baths are the one side systems only to eliminate the adsorption heats. So pressure lowering is necessary in desorption. In the some experiments even though temperature control systems were established, the hysteresis phenomenon occurred. It is considered that their causes arose from the insufficiency of the desorption heat supplying compared with the sufficiency of the adsorption heat eliminating because the heat pans were situated a little far from the adsorbents [Pierce et al., 1951]. In addition, the characteristic aspects for the hysteresis phenomenon are observed as follows.

In the research of Homes and Beebe [Homes and Beebe, 1957] the adsorbent of Shawiningan Acetylene Carbon Black did not show the hysteresis phenomenon for N_2, SO_2 and CO_2, but it did for NH_3. The authors observed that since the adsorbents did not have a larger radius than 25 Å, they did not show the hysteresis phenomenon in the desorption of N_2. But we think that since the bonding forces of all the former gases were very weak in the adsorptions and then the surface tensions were then also small, the supplies of the desorption heats were not necessary. And since the non-bonding pair electrons of the nitrogen in NH_3 were well attracted to the surface of the adsorbent and then made hydrogen bonding, and since surface tension existed strongly and the pores were well filled with NH_3 molecules, the hysteresis phenomenon occurred noticeably. There was no hysteresis phenomenon in the isotherms that NH_3 were adsorbed on the heat-treated adsorbent at 3,000 °C as shown in Figs. 5, 6 and 8 of the literature [Homes and Beebe, 1957]. The reason seems to be that since the adsorption sites of the adsorbent were much reduced and the bonding between the adsorbent and NH_3 was weak, the supply of desorption heat was not necessary.

It is seen from de Boer and Lippens's research [de Boer and Lippens, 1965] that the adsorption isotherms for the nitrogen molecules on the well crystallized boehmite show BET type and hysteresis. The authors observed that a meniscus could not be accomplished between the two parallel plates until the saturation vapor pressure was reached. The insufficiency of that explanation is that they did not consider the flat surface condensation adsorption. We think that the bohmite belongs to the non-porous adsorbent. That is verified that it has BET type adsorption isotherm. It is supposed that those condensation phenomena represent the dewdrops on the flat glass or the polished metal early in the morning. We think that the experiments which Barrer and Macleo [Barrer and Macleo, 1954] and Culver and Heath [Culver and Heath,1955] executed can be discussed in the same way. Since the attraction force of the nucleus of the adsorbent for the last layer molecule is tiny when x=1, the surface tension of the dewdrops is very weak. The surface tensions are overcome making the BET type hysteresis phenomenon. Therefore, hysteresis shows the finishing without the horizontal beginnings at the end of their isotherms.

From the experiment of water adsorption on Saran Charcoal by Darcy et al. [Darcy et al., 1958] it is seen that even if porous, the adsorbent did not show hysteresis. The authors explained that Saran Charcoal has too small pores for this to occur. But we think that a temperature controller possible to control as precisely as .002 °C was attached to the system and then the surface tension of the condensation film was well overcome when the adsorbates were desorbed, they were desorbed without pressure lowering with respect to the same amount of the adsorbed molecules. Hence there was no hysteresis phenomenon. Chuikina et al. [Chuikina et al., 1972] reached the same result.

The above hysteresis phenomena agree with Wooton and Brown's mention [Wooton and Brown, 1943] through the studies

of the other researchers that they disappeared in the adsorption-desorption by the temperature controller attached to the system.

Prenzlow and Halsey [Prenzlow and Halsey, 1957] did not mention the Bose-Einstein condensation and hysteresis phenomena for the adsorptions of Ar, O_2 and N_2 on graphitized carbon black at 65-80 K at all after xenon was pre-adsorbed on it. Generally, carbon black is supposed to have pores. Hysteresis would not occur owing to the precise temperature control even if they had executed the desorption experiment. First, when the argon gases were adsorbed on the adsorbent of bare p-33 (2700) which were not pre-adsorbed by xenon gas, the combined isotherms of type IV and type II of the free surface condensation isotherm (BET type), were shown in Fig. 1 of the literature [Prenzlow and Halsey, 1957]. Here the free surface means the flat surface which has adsorption sites at the outside of the pores. Hence the bare adsorbent had the adsorption sites at the inside and the outside of the pores. The first inflection point seems to be the point of the beginning of the Bose-Einstein condensation already; the second inflection point seems to be the midpoint of the pore condensation; and the third inflection point seems to be the point of free surface condensation occurring more after the pore filling condensation is completed. In Fig. 1 [Prenzlow and Halsey, 1957] the adsorption amount with respect to the relative vapor pressure is less flexible as the temperature increases. Its cause is because the atomic nucleus of the site as a vibrator has a higher vibration than it has at a low temperature and then reduces the adsorption. All the adsorption isotherms in Fig. 1 of the literature [Prenzlow and Halsey, 1957] with respect to the temperature have the same three inflection points. These isotherms seem to show the summed isotherms of Fig. 12 in the previous literature [Kim, 2000] and Fig. 17 in the present study. Fig. 2 of the literature [Prenzlow and Halsey, 1957] represents the summed isotherms of the isotherm of type V and the free surface condensation isotherm (BET type) of type II. The above interpretation about the temperature in Fig. 2 of the literature [Prenzlow and Halsey, 1957] is also valid. The adsorbent of type IV for the adsorption of argon was changed into the adsorbent of type V by the mono-layer pre-adsorption of xenon. The reason is because the surface mono-layer adsorption of argon became weak and xenon interfered with the adsorption of argon. The size of xenon is much larger than that of argon. Then the remaining sites after xenon was pre-adsorbed seem to adsorb argon unwillingly. Since the adsorbent on which xenon was pre-adsorbed had very small electro-negativity and did not have the adsorption force to adsorb argon nearly, D_{s1} or D_{s2} of β_{c1} or β_{c2} became smaller than D_{l1} or D_{l2}. In Figs. 1 and 2 of the literature [Prenzlow and Halsey, 1957] we understood that the figuring for the amount of the adsorbed argon was also appropriate to clarify the above matters. The characteristics of Bose-Einstein condensation of argon bring a larger cohesion force (D_{l1} or D_{l2}) than adhesion force (D_{s1} or D_{s2}). Even if the temperature is high in summer, the reason why it rains much at one time is because the condensation activation energy (E_∞, see below) is reduced and then the cloud is easily changed into rain by 2nd Bose-Einstein condensation when it contacts with the cold air. It is a unimolecular reaction and exothermic reaction that the cloud becomes rain. Then the condensation reaction rate constant can be expressed as $k=Ae^{-E_\infty/kT}$. If the condensation occurs quickly, the condensation heat should be eliminated as fast as possible. The high mountain and numerous

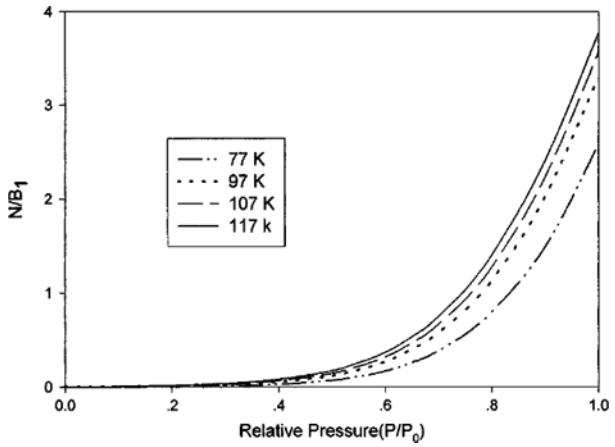

Fig. 18. Capillary condensational adsorption isotherms (Type V) Eq. (13) (j_{l1}/j_{s1}=1, $D_{l1}-D_{s1}$=1700 cal/g-mol, q=−25 cal/mol, m=.28, c_{c1}=.92, n=7) with respect to adsorption temperature.

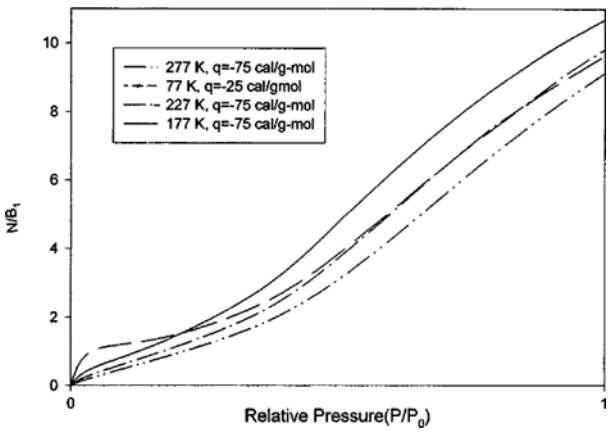

Fig. 19. Capillary condensational adsorption isotherms (Type IV) Eq. (13) (j_{l1}/j_{s1}=1, $D_{l1}-D_{s1}$=−1600 cal/g-mol, m=.28, c_{c1}= .92, n=7) with respect to various adsorption temperatures and additional energies.

trees there stagnate the cloud, eliminate the condensation heat of the cloud quickly, and heavy rain occurs easily. The more the temperature of the adsorption system increases, the more the adsorption amount increases (cf. Fig. 18). In the present study the adsorbents which describe the isotherm of type V are the materials containing carbon. The unknown aerosol which forms the cloud is known to include materials like carbonates. Carbon itself is hydrophobic. It is thus considered that since the pores of the carbonate adsorbents bring about the condensation adsorption of H_2O, they may be used in rainmaking.

Fig. 19 shows the capillary condensation adsorption isotherm of type IV [Eq. (13)] according to the various temperatures of the system and the various additional energies (q) in the nth layer.

CONCLUSION

The capillary condensation adsorption isotherms for the sites of two groups obtained in the present study agree well with the experimental data of type IV and type V, and also the capillary con-

densation adsorption isotherm on the sites of one group can be fitted to agree with the experimental data of type V. The surface areas obtained from the isotherm equation of type IV through the experimental data were much larger than those obtained from the BET equation and were fairly larger than those obtained from the experimental data by the authors. We could obtain the surface area through the experimental condensation adsorption data of type V. The pore radii obtained by using the capillary adsorption isotherm for the adsorbents causing the capillary condensation of type V were fitted well with those obtained from the Kelvin equation. The possible ranges of the layers used in optimizing Eqs. (13) and (28) according to the experimental data are broad. When the surface monolayer adsorption isotherms obtained appropriately with respect to the various adsorbents are compared with the x_B obtained from the BET equation, the error can be determined clearly. The hysteresis phenomena occurring between the adsorption and the desorption originate from the deviation of the thermodynamically reversible process between adsorption and desorption.

REFERENCES

Barrer, R. M. and Macleod, D. M., "Intercalation and Sorption by Montmorillonite," *Trans. Faraday Soc.*, **50**, 980 (1954).

Brunauer, S., Deming, L. S., Deming, W. E. and Teller, E., "On a Theory of the van der Waals Adsorption of Gases," *J. Am. Chem. Soc.*, **62**, 1723 (1940).

Brunauer, S., Emmett, P. H. and Teller, E., "Adsorption of Gases in Multimolecular Layers," *J. Am. Chem. Soc.*, **60**, 309 (1938).

Chuikina, V. K., Kiselev, A. V., Mineyeva, L. V. and Muttik, G. G., "Heats of Adsorption of Water Vapor on NaX and KNaX Zeolites at Different Temperatures," *J. Chem. Soc., Faraday Trans*, **1**, 1345 (1972).

Culver, R. U. and Heath, N. S., "Saran Charcoals," *Trans. Faraday Soc.*, **51**, 1569 (1955); *Chapter 4, in the below reference* (Gregg and Sing, 1969).

Darcey, J. R., Clunie, J. C. and Thomas, D. G., "The Adsorption of Water by Saran Charcoal," *Trans. Faraday Soc.*, **54**, 250 (1958).

de Boer, J. H. and Lippens, B. C., "Studies on Pore Systems in Catalysts II. The Shapes of Pores in Aluminum Oxide Systems," *J. Cat.*, **3**, 38 (1965).

Emmett, P. H. and Cines, M., "Adsorption of Argon, Nitrogen, and Butane on Porous Glass," *J. Phys. Chem.*, **51**, 1248 (1947).

Gregg, S. J. and Sing, K. S. W., "Adsorption, Surface Area and Porosity," Academic Press Inc. (London) Ltd., Second Printing (1969).

Harris, M. R. and Whitaker, G., "Surface Properties of Hydrolysed Titania. III*. Titania Prepared from Titanium Chloro-Alkoxides," *J. Appl. Chem.*, **13**, 348 (1963).

Hill, T. L., "Statistical Mechanics of Multimolecular Adsorption. I," *J. Chem. Phys.*, **14**, 263 (1946a).

Hill, T. L., "Theory of Multimolecular Adsorption from a Mixture of Gases," *J. Chem. Phys.*, **14**, 268 (1946b).

Homes, J. M. and Beebe, R. A., "Adsorption Studies on A Series of Heat Treated Shawiningan Acetylene Carbon Blacks," *Canadian J. of Chemistry*, **35**, 1542 (1957).

Katz, S. M., "Permanent Hysteresis in Physical Adsorption," *J. Phys. Chem.*, **53**, 1166 (1949).

Kim, D., "Statistically Modeled Adsorption Isotherms for the Multilayer Gas Molecules Adsorbed on Non-porous Solid Adsorbents of Two and Three Groups of Sites," *Korean J. Chem. Eng.*, **17**, 156 (2000).

Kipling, J. J. and Wilson, R. B., "Adsorptive Properties of Polymer Carbons," *Trans. Faraday Soc.*, **56**, 562 (1960).

Langmuir, I., "The Adsorption of Gases on Plane Surfaces of Glass Mica and Platinum," *J. Am. Chem. Soc.*, **40**, 1361 (1918).

Mason, G., "Determination of the Pore-size Distributions and Pore-space Interconnectivity of Vycor Porous Glass from Adsorption-desorption Hysteresis Capillary Condensation Isotherms," *Proc. R. Soc. Lond.*, **A 415**, 453 (1988).

McQuarrie, D. A., "Statistical Thermodynamics," Harper & Row Publisher (1979).

Pickett, G., "Modification of the Brunauer-Emmett-Teller Theory of Multimolecular Adsorption," *J. Am. Chem. Soc.*, **67**, 1958 (1945).

Pierce, C., Smith, R., Nelson, Wiley, J. W. and Cordes, H., "Adsorption of Water by Carbon," *J. Am. Chem. Soc.*, **73**, 4551 (1951).

Prenzlow, C. F. and Halsey, G. D. Jr., "Argon-Xenon Layer Formation on Graphitized Carbon Black from 65 to 80 K," *J. Phys. Chem.*, **61**, 1158 (1957).

Rao, K. S., "Hysteresis in Sorption. II," *J. Phys. Chem.*, **45**, 506 (1941).

Rudzinski, W. and Everett, D. H., "Adsorption of Gases on Heterogeneous Surfaces," Academic Press Ltd. (1992).

Salby, M. L., "Fundamentals of Atmospheric Physics," Academic Press, Chapter 9 (Fig. 9.14) (1996).

Sears, F. W. and Salinger, G. L., "Thermodynamics, Kinetic Theory and Statistical Thermodynamics," Addison-Wesley Publishing Company, 3rd ed. (1975).

Shull, C. G., "The Determination of Pore Size Distribution from Gas Adsorption Data," *J. Amer. Chem. Soc.*, **70**, 1405 (1948).

Wig, E. O. and Juhola, A. J., "The Adsorption of Water Vapor on Activated Charcoal," *J. Amer. Chem. Soc.*, **71**, 561 (1949).

Wooton, L. A. and Brown, C., "Surface Area of Oxide Coated Cathodes by Adsorption of Gas at Low Pressures," *J. Am. Chem. Soc.*, **65**, 113 (1943).